

Scanning near-field optic/atomic force microscopy in liquids

Hiroshi Muramatsu ^{a,*}, Norio Chiba ^a, Katsunori Homma ^a, Kunio Nakajima ^a, Tatsuaki Ataka ^a,
Satoko Ohta ^b, Akihiro Kusumi ^b, Masamichi Fujihira ^c

^a *Research Laboratory for Advanced Technology, Seiko Instruments Inc., Takatsuka-shinden, Matsudo-shi, Chiba 271, Japan*

^b *Department of Life Sciences, Graduate School of Arts and Sciences, The University of Tokyo, Meguro-ku, Tokyo 153, Japan*

^c *Department of Biomolecular Engineering, Tokyo Institute of Technology, Nagatsuta, Midori-ku, Yokohama 227, Japan*

Abstract

We report the performance of an optical fiber cantilever and the scanning near-field optical microscopy imaging of specimens in liquid. In our scanning near-field optical/atomic force microscope (SNOAM), the scanning of an optical fiber cantilever over the specimen was controlled by dynamic mode atomic force microscopy to reduce damage to the probe and soft specimens. The typical resonant frequency of the optical fiber cantilever was 25.6, while it was 29.5 kHz in the air. The Q factor of the cantilever depended on the vibration amplitude and showed typically 460–590 in the air and 65–270 in water. The relationship between the vibration amplitude and the average sample–probe separation indicated that the cantilever worked in the non-contact mode in water, while it worked in the cyclic-contact mode in the air. Cultured cells in aqueous solutions were visualized by the SNOAM, indicating that the SNOAM is suitable to observe soft specimens.

Keywords: Atomic force microscopy; Optical properties; Optical properties; Biomaterials

1. Introduction

Near-field optical microscopy in liquids has been long-awaited for the observation of specimens in aqueous media and organic solvents with high resolution. In biology, optical microscopy is essential for studying the structural basis of functions of cells and supramolecular complexes because it allows observation of their functional states in aqueous media. However, the resolution of conventional (far-field) optical microscopy is typically several hundred nanometers, which is insufficient for observing molecular events. Electron microscopes have much better resolution, but do not allow observation in aqueous solutions.

We previously developed a new scanning near-field optical microscope (scanning near-field optical/atomic force microscope (SNOAM)) in which a feedback signal from an atomic force microscope (AFM) in the dynamic mode was used to scan the probe tip along the surface contour of the sample [1,2]. An optical fiber with a sharp tip on one end was bent for use as a cantilever, and the a.c. amplitude of the cantilever deflection was held constant during scanning by moving the stage. If this system operates successfully in liquids, it will be good for soft samples and those with great variations in height, such as cultured cells. In this sense, for observation

of biological specimens, SNOAM may be superior to other systems that have been used in the atmospheric environment, such as those utilizing lateral shear force [3], scanning tunneling microscopy (STM) [4], and contact-mode AFM [5,6] as a method to control sample–tip separation. Tapping-mode AFM in liquids have been reported using flat-type cantilevers [7–9] although the optical fiber cantilever is round which helps to reduce viscositic resistance.

In the present investigation, we examine the performance of the optical fiber cantilever and observed specimens in liquids. Near-field images and AFM images (non-contact mode) were obtained simultaneously. This paper reports the performance of the optical fiber cantilever and the observation of a standard specimen in liquid and displays near-field optical images of cultured cells in an aqueous solution.

2. Experimental set-up

The SNOAM system is essentially the same as reported previously [2]. The optical-fiber cantilever is mounted on a bimorph and vibrated vertically against the specimen stage at the resonant frequency (typically 10–40 kHz). The vibration voltage applied on the bimorph was between 0.5 and 10 a.c. V. The vibration amplitude is monitored by detecting the deflection of the laser beam, which is reflected on the polished

* Corresponding author.

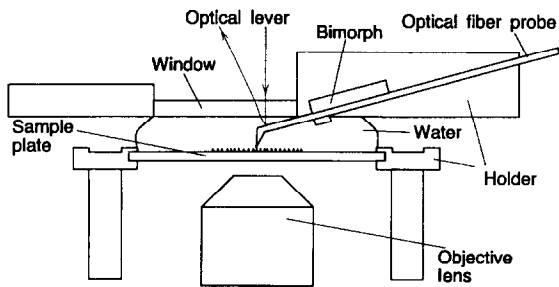


Fig. 1. Schematic diagram of the liquid cell in the SNOAM system.

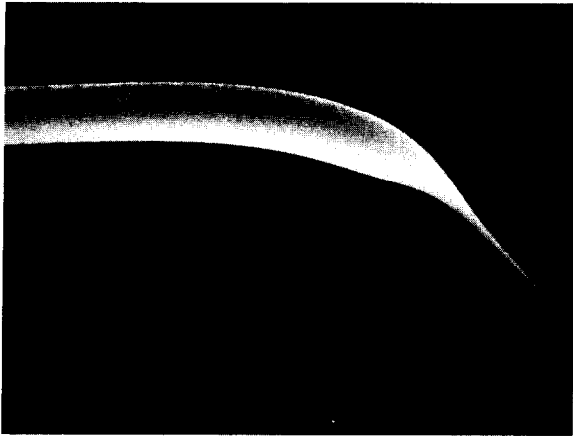


Fig. 2. A representative scanning electron microscope image of the probe made from an optical fiber coated with aluminum.

surface of the glass cantilever. The probe–sample distance is controlled dynamically by decreasing the vibration amplitude as the distance between the probe and the sample decreases.

Fig. 1 shows a liquid cell designed for the present experiment. Water and cell culture media were held between the glass plate and an upper window. Both the probe and the sample were immersed in solution.

The probe was prepared as described previously [2]. Briefly, an optical fiber was pulled with irradiation of a CO₂ laser to make a tip, and then bent with irradiation of a CO₂ laser. The probe was coated with 200 nm thick aluminum, and an aperture was made at the tip by chemical etching (Fig. 2).

3. Results and discussion

The spring constant of the probe was 2–20 N m⁻¹ as calculated on the basis of its shape (rod) and Young's modulus for quartz glass. Typically, the resonant frequency of the optical fiber tip cantilever was 29.6 kHz in the air. The resonant frequency decreased to 86% of 25.6 kHz. This frequency decrease can be explained by an addition mass of water to the cantilever. This addition mass is estimated as $\pi\rho r^2 l$ where ρ is viscosity of liquid, and r and l is radius and length of rod cantilever, respectively. As the resonant frequency is expressed roughly as $\omega = \sqrt{k/m}$, where m and k is the mass and spring constant of a vibrating material, respec-

tively, the ratio of the resonant frequency in water versus that in the air can be estimated using the addition mass of water as shown in the following equation.

$$\frac{\omega_{\text{water}}}{\omega_{\text{air}}} = \frac{\sqrt{k/(m_{\text{cantilever}} + m_{\text{water}})}}{\sqrt{k/m_{\text{cantilever}}}}$$

$$= \frac{\sqrt{\pi\rho_{\text{quartz glass}}r^2}}{\sqrt{\pi\rho_{\text{quartz glass}}r^2 + \pi\rho_{\text{water}}r^2}} = 0.83$$

where $\rho_{\text{quartz glass}}$ and ρ_{water} are 2.2 and 1.0 g cm⁻³ at 20 °C, respectively. This value (83%) agrees with the experimental result (86%).

Fig. 3 shows the relationship between the Q factor and the voltage applied on the bimorph to vibrate the cantilever. The Q factor is decreased by a factor of about 5–8 when the cantilever was immersed in water. The Q factor also depended on the vibration amplitude as shown in Fig. 3. This dependence is much larger in water than in the air. This is because the viscous resistance is larger in water than in the air, i.e. the kinematic viscosity of the air and water is 0.150 and 1.00 St at 20 °C, respectively. This Q factor is sufficient to operate non-contact mode AFM in water.

The a.c. voltage that must be applied to the bimorph to obtain a curve in water similar to that in air is greater by a factor of about 7 in water. The maximum vibration amplitude is proportional to the vibration voltage applied to the bimorph. With a decrease in the sample–probe separation, the vibration amplitude decreases as the probe approaches the sample at the extreme of each vibration cycle.

The relationship between the vibration amplitude of the cantilever and the average sample–probe distance was measured in air and water by varying the height of the specimen stage (Fig. 4). Fig. 4(a) shows that the amplitude decreases linearly in the air. A linear decrease of the vibration amplitude with lowering of the sample position outside the roll-out point is characteristic of the cyclic-contact mode AFM and indicates that cyclic-contact mode AFM operates normally in the air. The actual vibration amplitude can be estimated from this curve because the vibration amplitude decrease due to the decrease of vibration space of the probe, i.e. the distance between the roll-up point of the average sample–probe

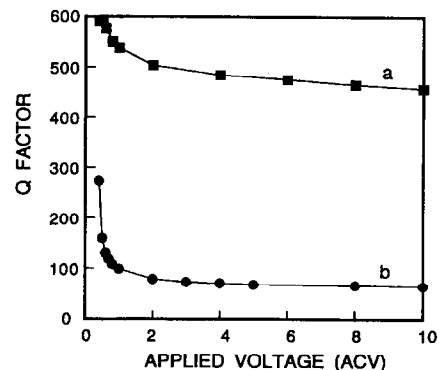


Fig. 3. Relationship between the Q factor of the optical fiber cantilever and the applied voltage to the bimorph for the cantilever vibration.

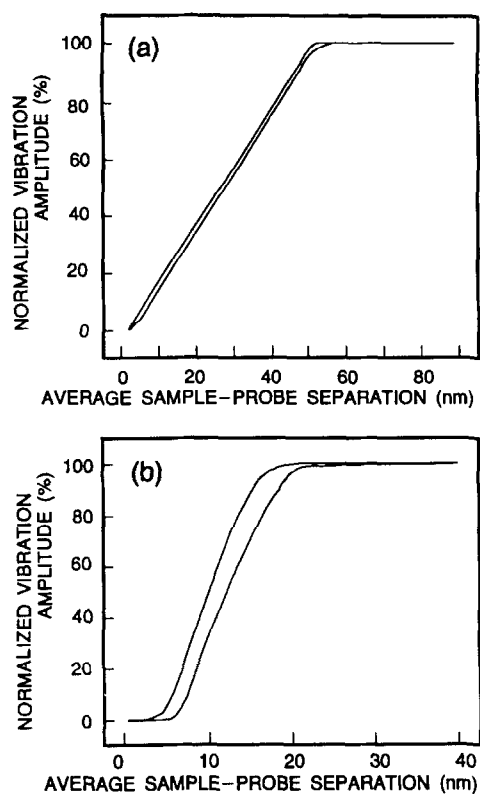


Fig. 4. Relationship between the vibration amplitude of the cantilever and the average sample-probe separation measured in air (a) and water (b). Vibration voltage of 1 a.c. V was applied and the vibration amplitude is estimated 100 and 20 for the air and water, respectively, from this relation.

separation and 0% point of that corresponds to the half of the actual vibration amplitude. In case of Fig. 4(a), the vibration amplitude was 100 nm for applying 1 a.c. V to the bimorph.

Fig. 4(b) shows that the amplitude decreases more gradually in water than in the air. A gradual decrease of the vibration amplitude with lowering of the sample position outside the roll-out point is characteristic of the non-contact mode AFM and indicates that non-contact mode AFM operates normally in water. The steep part of the curve indicates that the cantilever is in the cyclic contact (tapping) mode. The amplitude at the roll-out point is proportional to the vibration voltage between 1 and 10 a.c. V. The oscillation amplitude employed was between 20 and 200 nm (1–10 a.c. V for driving the bimorph) in water. The large oscillation amplitude is due to the long cantilever, which is 2–4 mm long, while normal cantilever probe for non-contact AFM is 100–500 μm long and shows a vibration amplitude of 10–20 nm in air.

Under typical imaging conditions, average sample-probe separation was controlled so that the amplitude of the vibration became 98% of the maximum vibration (when the probe was placed far away from the sample, the range of maximum vibration amplitude employed was between 20 and 200 nm). Therefore, the interaction force between the probe and the sample is likely to be as small as that for normal tapping mode AFM in water.

Fig. 5(a) and 5(b) show representative topographic and optical images of mouse keratinocyte cells in culture obtained

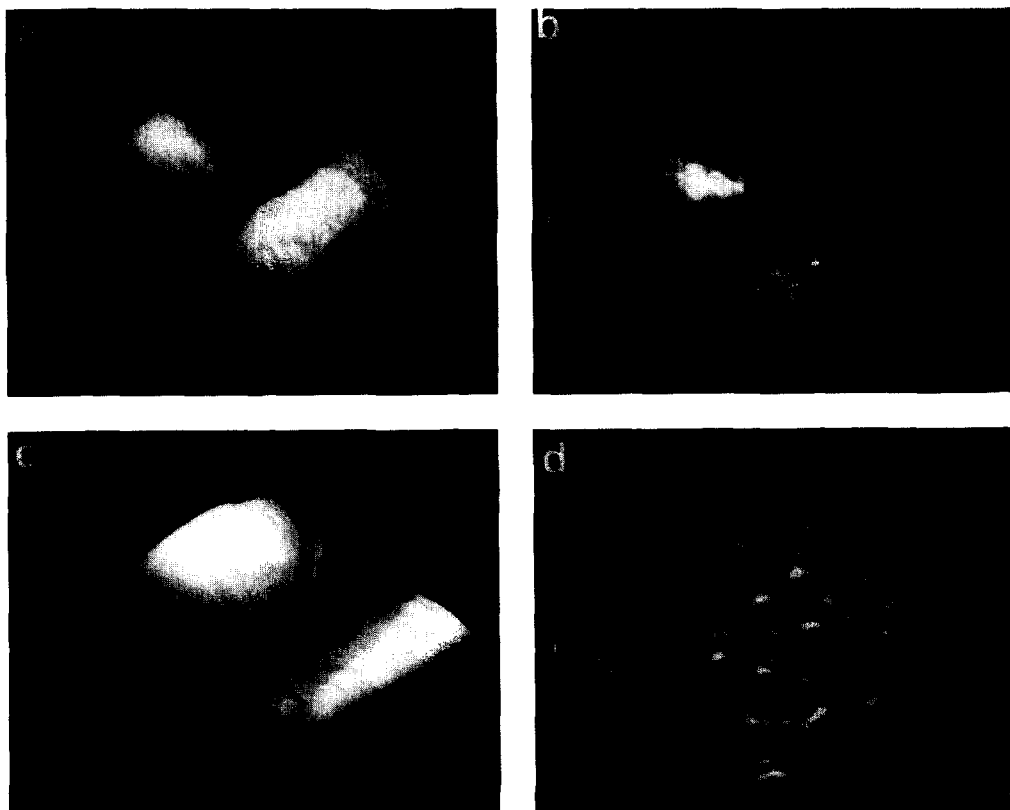


Fig. 5. Topographic ((a) and (c)) and near-field ((b) and (d)) images of cultured mouse keratinocytes in an aqueous solution. The cells were fixed by cross-linking with 2% paraformaldehyde. The areas imaged are 20 μm \times 20 μm ((a) and (b)) and 10 μm \times 10 μm ((c) and (d)).

simultaneously with the non-contact AFM mode and near-field optical transmission mode. This cell line was obtained from Dr. S. Yuspa at the National Cancer Institute, and was cultured on a 5 mm × 5 mm cover slip as described previously [10,11]. The cells were fixed with 2% paraformaldehyde before SNOAM observation. The overall topography of the cell in lower magnification (Fig. 5(a)) is similar to that obtained for living keratinocytes as observed by contact-mode AFM in cell culture medium [12]. The outer edges of the cells coincided in the near-field and non-contact mode AFM topographic images, while the fine structures observed in the near-field image showed no correlation with the topographic image.

Fig. 5(c) and 5(d) show the images at a higher magnification. The near-field image (Fig. 5(d)) shows many filamentous structures in the cell, while the topographic image is insensitive to such structures. We examined various types of other cells, including normal rat kidney (NRK) fibroblasts, leaf cells of box wood, *E. coli*, etc. The near-field images of NRK cells showed the presence of various filaments in the cell, while the latter two did not. The general feature of the filaments of NRK cells are different from those seen in keratinocytes shown in Fig. 5(d). In some images of keratinocytes, these filaments merge with thicker filaments, which are splaying out from the near-nuclear region toward the cell borders. Similar structures were also observed in the contact-mode AFM images.

These filaments are difficult to observe in normal Nomarski and phase-contrast optical microscopy due to the lower resolution and contrast. The nature of these filaments is currently being investigated. Since they do not look like stress fibers (straight actin bundles), near-field microscopy may have selectively imaged the filaments near the apical surface of the cell.

Various filaments inside living cells can be visualized from outside the cells using the contact-mode AFM, while topographic images of the cell by SNOAM (Fig. 5(a) and 5(c)) exhibited only the surface of the cell. This result further

demonstrated that the force exerted on the cell membrane is substantially weak.

Thus, SNOAM introduces a new method for studying cellular structures in living cells at a resolution and contrast unobtainable by conventional optical microscopy. This technique may reveal cell characteristics hitherto undetected by optical microscopy of living cells or electron microscopy of processed cells. In addition, the present study suggests that the SNOAM system is widely applicable to specimens in water and other fluid media.

Acknowledgements

This study was supported in part by Special Coordination Funds from the Science and Technology Agency of the Japanese government.

References

- [1] H. Muramatsu, N. Chiba, T. Ataka, H. Monobe and M. Fujihira, Proceeding of Second Conference on Near-field Optics, Raleigh, NC, 20–22 October 1993, *Ultramicroscopy*, 57 (1995) 141.
- [2] N. Chiba, H. Muramatsu, T. Ataka and M. Fujihira, *Jpn. J. Appl. Phys.*, 34 (1995) 321.
- [3] E. Betzig and J.K. Trautman, *Science*, 257 (1992) 189.
- [4] U.T. Dürig, D.W. Pohl and F. Rohner, *J. Appl. Phys.*, 59 (1986) 3318.
- [5] S. Shalom, K. Lieberman and A. Lewis, *Rev. Sci. Instrum.*, 63 (1992) 4061.
- [6] N.F. van Hulst, M.H.P. Moers, O.F.J. Noordman, R.G. Tack, F.B. Segerink and B. Bölger, *Appl. Phys. Lett.*, 62 (1993) 461.
- [7] P.K. Hansma, J.P. Cleveland, M. Radmacher, D.A. Walters, P.E. Hillner, M. Bezanilla, M. Fritz, D. Vie and H.G. Hansma, *Appl. Phys. Lett.*, 64 (1994) 1738.
- [8] C.A.J. Putman, K.O. Van der Werf, B.G. De Grooth, N.F. Van Hulst and J. Greve, *Appl. Phys. Lett.*, 64 (1994) 2454.
- [9] M. Dreier, D. Anselmetti, T. Richmond, U. Dammer and H. J. Güntherodt, *J. Appl. Phys.*, 76 (1994) 5095.
- [10] M. Kulesz-Martin, A.E. Kilkenny, K.A. Holbrook, V. Digernes and S.H. Yuspa, *Carcinogenesis (London)*, 4 (1983) 1367.
- [11] A. Kusumi, Y. Sako and M. Yamamoto, *Biophys. J.*, 65 (1993) 2021.
- [12] M. Takeuchi, H. Miyamoto, H. Komizu and A. Kusumi, *Cell Struct. Funct.*, 17 (1992) 487.